



**High temperature thermal conductive nanocomposite textile  
by “green” electrospinning**

Journal:	<i>Nanoscale</i>
Manuscript ID	NR-ART-06-2018-005167.R1
Article Type:	Paper
Date Submitted by the Author:	19-Jul-2018
Complete List of Authors:	<p>Wang, Jiemin; Deakin University, Institute for Frontier Materials          Li, Quanxiang; Deakin University, Engineering          Liu, Dan; Deakin University, Institute for Frontier Materials          Chen, Cheng; Fuzhou University, ; Deakin University School of Life and Environmental Sciences,          Chen, Zhiqiang; Deakin University, Institute for Frontier Materials          Hao, Jian; Jiangsu Normal University, School of Physics and Electronic Engineering          Li, Yinwei; Jiangsu Normal University, School of Physics and Electronic Engineering          Zhang, Jin; Institute for Frontier Materials, Deakin University          Naebe, Minoo; Deakin University, Engineering          Lei, Weiwei; Deakin University, Institute for Frontier Materials</p>



## Journal Name

## Article

## High temperature thermal conductive nanocomposite textile by “green” electrospinning

Received 00th January 20xx,  
Accepted 00th January 20xx

DOI: 10.1039/x0xx00000x

www.rsc.org/

Jiemin Wang,<sup>†a</sup> Quanxiang Li,<sup>†a</sup> Dan Liu,<sup>a,\*</sup> Cheng Chen,<sup>a</sup> Zhiqiang Chen,<sup>a</sup> Jian Hao,<sup>b</sup> Yinwei Li,<sup>b</sup> Jin Zhang,<sup>a</sup> Minoo Naebe,<sup>a</sup> Weiwei Lei<sup>a,\*</sup>

Recently, thermal regulated textiles have attracted wide interest owing to the ability to realize personal cooling and provide thermal comfort. However, most of thermal conductive textiles cannot afford higher temperature (>200°C), which restricts the further applications in aviation, fire extinguishing or military requiring high temperature heat spreader. Here, we report a high temperature thermal conductive nanocomposite textile consisting of amino functional boron nitride nanosheets (FBN) and polyimide (PI) nanofibers. Notably, the textile is “green” electrospun from aqueous solution without any organic solvents, which is facile, economic and environmental. Moreover, both FBN and the precursor of PI are modified to be water soluble and exhibit good compatibility in the spinning solution even under high concentration. The “green” method obtained FBN-PI textile shows high thermal conductivity ( $13.1 \text{ W m}^{-1} \text{ K}^{-1}$ ) at high temperature (300 °C), filling in the gap of thermal conductive polymer nanocomposite fiber for high temperature thermal regulation. Furthermore, it also provides efficient cooling capability as thermal spreader. The good performance ascribes to the weaving of the aligned FBN filament in the thermal stable PI fiber, which constructs effective thermal conductive network. In addition, the nanocomposite textile is lightweight, soft and hydrophobic, which is promising for electronic packaging or space suit for special high temperature thermal management.

### Introduction

Wearable textiles with thermal regulation capacity have attracted wide attention because of the potential to adjust the body temperature and provide thermal comfort.<sup>1,2</sup> Among them, thermal

conductive textiles are one of the most promising thermal regulated textiles for effective thermal management. Especially through direct heat conduction and spread of the fiber, it enables personal cooling in hot weather or during sports efficiently.<sup>3</sup> Up to now, most reported thermal conductive textiles consist of polymer matrix and high thermal conductive boron nitride (BN) nanosheets fillers.<sup>3-6</sup> By improving the compatibility or orientation of the BN nanosheets in the polymer matrix, the textiles could achieve satisfactory thermal conductivities.

Although much efforts have been dedicated to improve the thermal conductivities of the fibres, the issue still remains that most thermal conductive textiles with conventional polymers cannot afford higher temperature (>200°C),<sup>3,5,7,8</sup> thereby impeding the further applications in some industries such as aviation, fire extinguishing or military requiring high temperature heat spreader. Unlike some water-soluble polymers such as polyvinyl alcohol (PVA) with soft linear chains and hydroxyl groups,<sup>3,4,9</sup> the high temperature resistance polymers such as polyimide (PI) with benzene rings and rigid chains can hardly interact with BN nanosheets in organic solvents,<sup>10-14</sup> leading to nonuniform dispersibility and compatibility of BN nanosheets in the spinning solution, thus restraining the final thermal properties. In addition, the organic spinning solutions such as dimethylacetamide (DMAc), methyl-2-pyrrolidinone (NMP) or dimethylsulfoxide (DMSO) for those high temperature resistance polymers are toxic, which are not environment-friendly during mass production.<sup>6,15-18</sup>

Here, for the first time, we have developed a high temperature thermal conductive textile based on functional BN nanosheets (FBN) and PI nanocomposite fibers by a “green” electrospinning method via aqueous solution. The FBN nanosheets, functionalized with amino group are highly dispersible in water.<sup>9,19,20</sup> In addition to this, the precursor of PI, is also designed to be water soluble with ammonia salt modification in the side chains.<sup>18,21</sup> Through the balance force of hydrogen bonding interaction, charge repulsion and  $\pi$ - $\pi$  attraction, the FBN nanosheets could be well compatible with PI

<sup>a</sup> Institute for Frontier Materials, Deakin University, Waurn Ponds Campus, Locked Bag 20000, Victoria 3220, Australia.

<sup>b</sup> School of Physics and Electronic Engineering, Jiangsu Normal University, Xuzhou, Jiangsu, 221116, China

<sup>†</sup> J. Wang and Q. Li have contributed equally.

Electronic Supplementary Information (ESI) available: details of any supplementary information available should be included here. See DOI: 10.1039/x0xx00000x

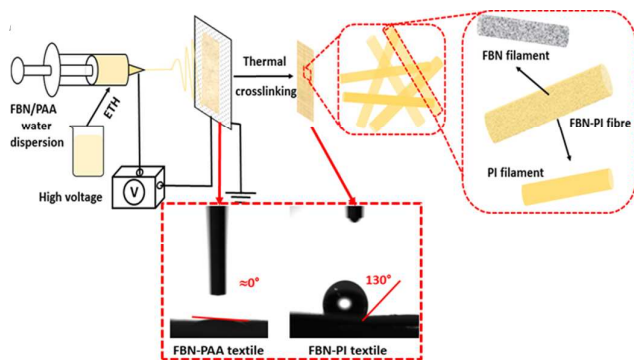


**Fig 1.** The schematic illustration of “green” electrospinning process for producing FBN-PI textile.

precursors in water at high concentration without precipitation. After electrospinning, the FBN is spun into filament in the fiber, thus constructing effective thermal conductive network. The as-obtained nanocomposite textile is soft, lightweight, hydrophobic and wearable, exhibiting outstanding cooling ability as heat spreader. Meanwhile, it shows high thermal conductivity (TC) of  $13.1 \text{ W m}^{-1} \text{ K}^{-1}$  at  $300 \text{ }^\circ\text{C}$ , which is promising for the applications of high temperature thermal regulated textiles.

## Experimental section

**Preparation of functional boron nitride (FBN) nanosheets.** Typically, h-BN (Momentive Performance Materials, Inc.) and urea (Sigma-Aldrich) were mixed in a steel milling container using a planetary ball mill (Pulverisette 7, Fritsch). The mixture with a weight ratio of 1:20 (h-BN: urea) was protected by nitrogen and milled at a rotation speed of 500 r.p.m. for 20 h. The obtained powders were dissolved in water and dialyzed for 1 week in deionized water to remove the urea, yielding stable aqueous dispersions of FBN nanosheets.

**Preparation of water-soluble polyimide (PI) precursor.** The 4, 4'-diaminodiphenyl ether (4,4'-ODA, Sigma-Aldrich) was dissolved in DMAc firstly. Then, a quantity of pyromellitic dianhydride (PMDA, Sigma-Aldrich) was dissolved into the mixture with mechanical stirring for 24 h under  $\text{N}_2$  protection to obtain poly (amic acid) (PAA) solution. The PMDA/4, 4'-ODA molar ratio was 100:99. The resultant solution was poured into excessive deionized water, and the corresponding precipitate was filtrated, washed, and dried to move the residual deionized water. After that, the triethylamine (TEA) (Sigma-Aldrich) and deionized water was added to dissolve the dried PAA. After reaction for 10 h at room temperature, the water-soluble polyimide precursor solution was obtained.

**Preparation of FBN/PI textiles.** FBN-PI textiles were fabricated by electrospinning and thermal crosslinking. The FBN water dispersion was firstly concentrated. And then it was mixed with PAA solution to form viscous mixture. Afterwards, some ethanol was added, and the mixtures were magnetically stirred for 1 h. The electrospinning was conducted in air. Firstly, the electrospinning solution was loaded into a plastic syringe equipped with 23 gauge stain needle. The flow rate was fixed at 2 ml/h by a syringe pump (KDS 200, KD Scientific Inc.). A high-voltage (20 kV) and a flate plate was used in

the electrospinning with a surface linear speed of  $\sim 16.8 \text{ m/s}$ . The distance between the tip and the collector was 15 cm. After that, the FBN-PAA fibre mats were thermal-crosslinked in tube furnace under  $\text{N}_2$  protection at  $80 \text{ }^\circ\text{C}$ ,  $150 \text{ }^\circ\text{C}$ ,  $170 \text{ }^\circ\text{C}$  for 1 hour respectively and finally  $300 \text{ }^\circ\text{C}$  for 2 hours.

**Material characterization and measurement.** XRD measurements were performed on a PANalytical X'Pert PRO apparatus operating with  $\text{Cu K}\alpha$  radiation. The FTIR spectrum were recorded using a Nicolet 7199 FTIR spectrometer. Contact angle measurements were obtained on a contact angle goniometer (CAM101, KSV), SEM imaging and EDS mapping were performed on a Zeiss Supra 55 VP SEM instrument. TEM and HRTEM imaging were performed on a JEOL 2100F microscope operating at 200 kV. The mechanical testing was performed by a universal testing machine (Instron 30 KN tentile tester) by using a 50-N load cell with a loading rate of 5 mm/min. The thermal behavior was analyzed using TGA on a TA Instruments Q50 TGA thermal analyzer at a heating rate of  $10 \text{ }^\circ\text{C min}^{-1}$  from room temperature to  $800 \text{ }^\circ\text{C}$  under 60 sccm compressed air flow. Specific heat was measured by using the differential scanning calorimetry (DSC Q200, TA Instruments). The thermal diffusivity of nanocomposite membranes (diameter of 25.4 mm) were measured from 30-300  $^\circ\text{C}$  with an LFA 457 analyzer (NETZSCH, Germany) via using different modules. The thermal conductivities of the nanocomposite membranes was calculated according the equation:  $\text{TC} = \alpha \times \rho \times C$ , where  $\alpha$ ,  $\rho$ , and  $C$  correspond to the thermal diffusivity, density, and specific heat capacity of the tetxile membranes. The specific heat capacity is measured by Differential scanning calorimetry (DSC Q200, TA Instruments). The heat capacity of the nanocomposite is calculated according to the equitation:  $C_p = C_{pr}\Phi + C_{pm}(1-\Phi)^{10}$ , where  $C_p$  is the specific heat capacity of the whole electrospinning nanofibre mats and  $C_{pr}$  is the specific heat capacity of the filler (BNNS), and  $C_{pm}$  is the specific heat capacity of the matrix (PI). While  $\Phi$  is the volume fraction of BNNS. The thermal infrared images are captured by FLIR T1040 camera.

## Results and discussion

The “green” electrospinning process is briefly illustrated in **Fig.1**. For the preparation of the aqueous spinning solution. Firstly, the precursor of PI, namely poly (amic acid) (PAA) was modified to be water soluble by introducing of triethylamine (TEA) (Scheme. S1).<sup>18,21</sup> Meanwhile, the amino functional BN nanosheets (FBN) water dispersion is highly concentrated to  $30 \text{ mg ml}^{-1}$  as shown in **Fig. 2**. From FTIR and XPS results (Fig.S2 and S3), the amino group was successfully functionalized into the BN nanosheets after ball milling with urea.<sup>19</sup> The lateral size of the FBN is around 100-200nm with 3-6 layers lamella as previously reported.<sup>9,19,20</sup> Notably, the great hydrophilicity of the FBN benefits the good dispersibility and compatibility with TEA modified PAA in water. Furthermore, through the synergetic effect of hydrogen bonding force between amino group of FBN and amino/imine containing groups in the PAA chains, electrostatic repulsions of FBN and PAA  $\pi$ - $\pi$  attraction between the boron-nitride layer conjugation and benzene ring in the polymer backbone, the FBN can well interact with PAA in water, thus resulting

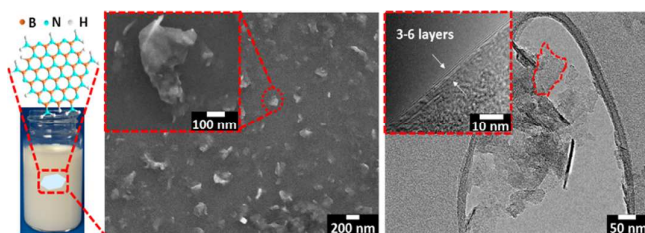


**Fig 2.** The optical image of FBN water dispersion and SEM, TEM images of FBN nanosheets.

in homogenous aqueous spinning solution. In addition, despite the high concentration of FBN ( $30\text{mg ml}^{-1}$ ), there is no aggregation or precipitation in the FBN/PAA mixture water solution even after several days, demonstrating the impressive miscibility as well as guaranteeing the viscosity for spinning. The as-obtained FBN-PAA nanofiber membrane could be continuously electro-spun from the aqueous liquid. During spinning, apart from some added ethanol (ETH) for faster evaporation of solvents, no toxic organic reagents such as DMAc and NMP are used, which is green and eco-friendly compared with traditional PI electrospinning.<sup>6,15-17</sup> After that, the textile membrane is peeled off from the aluminum foil. Finally, the FBN-PI nonwoven fabric consisting of both FBN and PI filament is achieved after further thermal crosslinking. The contact angle of FBN-PAA textile approaches  $0^\circ$ , further suggesting the hydrophilicity. Whereas it becomes hydrophobic (contact angle  $\approx 130^\circ$ ) after thermal transferring to FBN-PI fabric (Fig. 1). The hydrophobicity is considered to enable the washable textiles, which would not be soluble in water. **Fig. 3a** illustrates the optic photos of the FBN-PI textiles with different shapes. The textile fabric is so light and highly flexible that can undertake any bending, folding and deforming. Fig. 3b presents the typical SEM morphology of the FBN-PI textiles. After electrospinning, the fibers are self-entangled with diameters of 400 nm. Interestingly, like pure PI fiber (Fig. S4), the surface of the nanocomposite fibre is mostly smooth without FBN fragments attached (Fig. 3b inset), implying that the FBN may fuse with the PI together. This is demonstrated by TEM images (Fig. 3c and Fig. S5). Obviously, the FBN lamella are vertically aligned and uniformly dispersed in the PI matrix. It discloses that the aqueous mixing could successfully generate the super compatible structure between FBN and PI. Different from previously reported common BN/polymer textiles, in which large BN flakes are either tightly attached or randomly distributed on the surface of the polymer fibre,<sup>4,6,22</sup> this obtained nanocomposite fibre shows high homogeneity with interfused FBN and PI filaments. The good compatibility originates from the excellent water solubility and intimate interaction between each other.<sup>9,20</sup> The energy dispersive spectrometer (EDS) mapping in Fig. 3d further suggests that the carbon (C), oxygen (O), boron (B) and nitrogen (N) elements are evenly distributed in the nanocomposite textiles. And it is more convincing that a large area of textiles is marked with mapping rather than one single fibre here to disclose the uniformity. The XRD and FTIR results of the composite fibre also show the characteristic bands of FBN in the spectrum (Fig. S6), akin to that of FBN/polymer

membranes.<sup>9,20</sup> In addition, the TGA test indicates that there is 20 wt% of FBN in the nanocomposite (Fig. 3e).

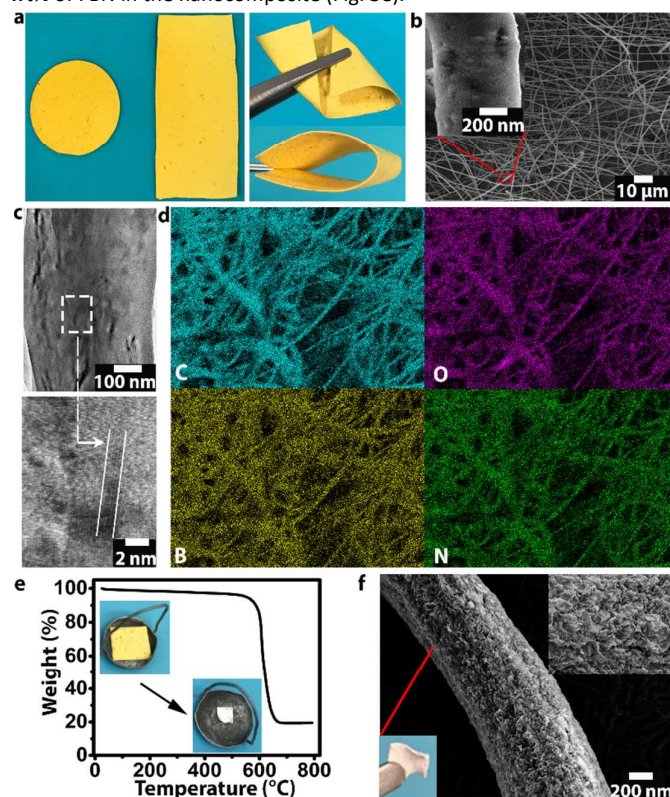


**Fig 3.** The morphology and structure of FBN-PI textile. (a) The optical photos of the flexible and foldable FBN-PI textile. (b) The SEM images of FBN-PI nanofiber textile mat (surface area), and the inset shows the single nanofiber morphology from the textile. (c) The TEM images of FBN-PI fibre. (d) The EDS mapping of FBN-PI fibre. (e) The TGA curve of FBN-PI textile fabric. The inset shows the optical topography of the fabric before and after TGA. (f) The SEM image of FBN filament after TGA test. The inset (left) shows the optical topography of the FBN fabric. The inset (right) shows the magnified SEM image of FBN nanosheets stacking.

And the neat intact FBN fabric rather than loose powders or bulk agglomerated pieces after TGA could be observed (Fig. 3e inset). Although the pure BN materials are so brittle and fragile when deformed, the neat FBN textile still remains curved shape without damage, highlighting the FBN fibre network throughout the nanocomposite textile. By comparing the XRD patterns (Fig. S7), it could be seen that the (002) peak of FBN-PI textile shifts to a higher diffraction angle with largely reduced intensity, indicating that, in the FBN-PI textiles, the spacing between the layers of FBN slightly decreases owing to the incorporation of PI chains, which demonstrates the good compatibility and interaction between FBN and PI. The results also well corresponding to the TEM analysis. In fact, the contents of FBN and PAA could be arbitrarily tuned in the water solution due to the super compatibility. Nevertheless, due to the mechanical limitation of FBN as nanofiber, we adapt 20 wt% of FBN in the nanocomposite textile, which still keep good stretching stress and elongation compared to pure PI textile (Fig. S8). The

morphology of FBN architecture in the textiles after TGA is displayed in Fig. 3f. It could be seen that the FBN nanosheets are closely stacked and arranged like squama to form the fibre-shape filament.

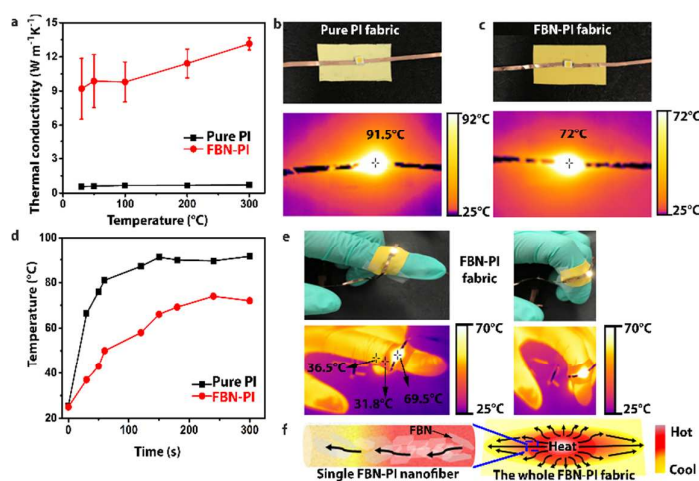


**Fig 4.** Application of FBN-PI textile as wearable thermal regulated textile. (a) Temperature-dependent TCs of FBN-PI and pure PI textile, respectively. (b) Optical and corresponding IR image of pure PI fabric as LED heat spreader (c) Optical and corresponding IR image of FBN-PI fabric as LED heat spreader. (d) The relationship between temperature and heating time for FBN-PI and pure PI fabrics, respectively. (e) The images of wearable FBN-PI fabric as heat dissipation spreader between LED and finger. (f) The mechanism of heat transfer in the FBN-PI fabric.

The small dimension of FBN nanosheets also facilitates the configuration without block deposition. Moreover, there are large contact areas between intimately overlaid FBN nanosheets, constructing the effective thermal transfer route and keep the pure FBN fabric shape compact. Meanwhile, through electrospinning, the stacked FBN nanosheets can be aligned and highly oriented in the filament, which are expected to efficiently improve the TC along the single fibre microscopically, in spite of some macroscopic twisting of fibres in Fig. 3b.

The thermal conductive performance of the FBN-PI textiles is shown in Fig. 4. There is a remarkable increase of TCs in the parallel direction from 30 °C to 300 °C (Fig. 4a). With a low FBN loading of 20 wt% (12.5 vol%), the TC of the electro-spinning FBN-PI textile mat reaches the value of  $13.1 \text{ W m}^{-1} \text{ K}^{-1}$  at 300 °C, corresponding to an enhancement of 4773% compared with pure electrospinning PI textile mat. And the thermal conductivity remains no change even after 3 cycles (Fig. S9), illustrating the good thermal conductive performance and stability. It contributes to the successful weaving of the aligned FBN filament in the nanocomposite fiber. More importantly, it is the first time to report thermal conductivity at such a high temperature for polymer nanocomposite textiles, addressing the gap for high temperature thermal conductive textiles for thermal regulation. To further study the heat diffusion and cooling capacity, a LED is placed on the surface of pure PI textile and FBN-PI textile, respectively. (Fig. 4b

and c). Then the LED is lightened to generate heat through the chip. After 5 minutes of lighting, one can see that the central temperature of pure PI textile reaches 91.5 °C. While it only attains 72 °C for FBN-PI textile, indicating the efficient heat spreading through the FBN filament network. Fig. 4d exhibits the heating rate of two textiles. Obviously, the FBN-PI textiles show a much lower heating rate owing to the effective thermal diffusion, confirming the efficient cooling and thermal regulation. Furthermore, as wearable textile, the FBN-PI fabric could be tied around the finger, with stretching and folded flexibly (Fig. 4e). It is impressive that the nanocomposite textiles efficiently afford the heat dissipation between LED and finger. Although the central LED temperature is 69.5 °C, the finger is not warmed and keeps the normal body temperature of 36.5 °C. While the surface temperature of the textile only reaches 31.8 °C, lower than both LED and finger temperatures. The heat spread mechanism is illustrated in Fig.4f. From the macroscopical view, the heat spread from central thermal sources (hot spot: lighted LED) to circumjacent direction (See below), this is demonstrated in the IR image (Fig.4c). While from the microscopic view, the heat transfers effectively in one single nanofiber (see below) owing to the closely stacked FBN filament (Fig.3f), which constructs the effective thermal conductive network (Fig.3f), which constructs the effective thermal conductive network. The results demonstrate the excellent cooling behavior ascribing to the FBN filament thermal conduction in the fibre. Hence the novel thermal conductive FBN-PI textiles place high potential value for high temperature thermal regulated clothing in the industrial application.

## Conclusions

In conclusion, a facile, effective and environment friendly route was designed to prepare high temperature thermal textiles. The highly water-soluble FBN nanosheets are well compatible with the modified PI precursor in aqueous solution, which provides prerequisite for further green electrospinning. The as-obtained FBN-PI textile is lightweight, soft and hydrophobic. More importantly, for the first time, it shows high thermal conductivity ( $13.1 \text{ W m}^{-1} \text{ K}^{-1}$ ) at high temperature (300 °C), filling in the gap of thermal conductive polymer nanocomposite fiber for high temperature thermal regulation. Moreover, the FBN nanosheets are packed closely to form aligned filament in the nanocomposite fibre during electrospinning, thus constructing effective thermal conductive networks for the heat transport. To summarize, the novel green aqueous solution derived thermal conductive textiles provide new insight for effective heat dissipation and cooling at high temperature, which could be applied in the electronic packaging or space suit that has special temperature requirement.

This work was financially supported by the Australian Research Council Discovery Early Career Researcher Award scheme (DE150101617 and DE140100716), and Deakin University Central Research Grants Scheme.

## Notes and references

- 1 P. Hsu, A. Song, P. B. Catrysse, C. Liu, Y. Peng, J. Xie, S. Fan and Y. Cui, *Science*, 2016, **353**, 1019-1023.
- 2 P. Hsu, C. Liu, Alex Y. Song, Z. Zhang, Y. Peng, J. Xie, K. Liu, C. Wu, P. B. Catrysse, L. Cai, S. Zhai, A. Majumdar, S. Fan and Y. Cui, *Science Advances*, 2017, **3**, e1700895.
- 3 T. Gao, Z. Yang, C. Chen, Y. Li, K. Fu, J. Dai, E. M. Hitz, H. Xie, B. Liu, J. Song, B. Yang and L. Hu, *ACS Nano*, 2017, **11**, 11513-11520.
- 4 J. Chen, X. Huang, B. Sun, Y. Wang, Y. Zhu and P. Jiang, *ACS Appl. Mater. Interfaces*, 2017, **9**, 30909-30917.
- 5 T. Terao, C. Zhi, Y. Bando, M. Mitome, C. Tang and D. Golberg, *J. Phys. Chem. C*, 2010, **114**, 4340-4344.
- 6 J. Gu, Z. Lv, Y. Wu, Y. Guo, L. Tian, H. Qiu, W. Li and Q. Zhang, *Compos Part A: Appl. Sci. Manufac.* 2017, **94**, 209-216.
- 7 C. Lu, S. W. Chiang, H. Du, J. Li, L. Gan, X. Zhang, X. Chu, Y. Yao, B. Li and F. Kang, *Polymer*, 2017, **115**, 52-59.
- 8 A. Yang, L. Cai, R. Zhang, J. Wang, P. C. Hsu, H. Wang, G. Zhou, J. Xu and Y. Cui, *Nano Lett*, 2017, **17**, 3506-3510.
- 9 J. Wang, Y. Wu, Y. Xue, D. Liu, X. Wang, X. Hu, Y. Bando and W. Lei, *J. Mater. Chem. C*, 2018, **6**, 1363-1369.
- 10 M. Tanimoto, T. Yamagata, K. Miyata and S. Ando, *ACS Appl. Mater. Interfaces*, 2013, **5**, 4374-4382.
- 11 M. Naebe, J. Wang, Y. Xue, X. Wang and T. Lin, *J. Appl. Polym. Sci.*, 2010, **118**, 359-365.
- 12 Y. Chen, X. Gao, J. Wang, W. He, V. V. Silberschmidt, S. Wang, Z. Tao and H. Xu, *J. Appl. Polym. Sci.*, 2015, **132**, 41889.
- 13 T. Wang, M. Wang, L. Fu, Z. Duan, Y. Chen, X. Hou, Y. Wu, S. Li, L. Guo, R. Kang, N. Jiang and J. Yu, *Sci Rep*, 2018, **8**, 1557.
- 14 S. Zhang, X. Li, X. Guan, Y. Shi, K. Wu, L. Liang, J. Shi and M. Lu, *Compos. Sci. Technol.*, 2017, **152**, 165-172.
- 15 J. Gong, Z. Liu, J. Yu, D. Dai, W. Dai, S. Du, C. Li, N. Jiang, Z. Zhan and C.T. Lin, *Compos Part A: Appl. Sci. Manufac.*, 2016, **87**, 290-296.
- 16 Q. Liu, Y. Wang, L. Dai and J. Yao, *Adv Mater*, 2016, **28**, 3000-3006.
- 17 Q. Wang, W.-L. Song, L. Wang, Y. Song, Q. Shi and L. Z. Fan, *Electrochim. Acta*, 2014, **132**, 538-544.
- 18 S. Jiang, H. Hou, S. Agarwal and A. Greiner, *ACS Sustain. Chem. Eng.*, 2016, **4**, 4797-4804.
- 19 W. Lei, V. N. Mochalin, D. Liu, S. Qin, Y. Gogotsi and Y. Chen, *Nat Commun*, 2015, **6**, 8849.
- 20 Y. Wu, Y. Xue, S. Qin, D. Liu, X. Wang, X. Hu, J. Li, X. Wang, Y. Bando, D. Golberg, Y. Chen, Y. Gogotsi and W. Lei, *ACS Appl. Mater. Interfaces*, 2017, **9**, 43163-43170.
- 21 Y. Qin, Q. Peng, Y. Ding, Z. Lin, C. Wang, Y. Li, F. Xu, J. Li, Y. Yuan, X. He and Y. Li, *ACS Nano*, 2015, **9**, 8933-8941.
- 22 S. Nagarajan, H. Belaid, C. Bohatier, C. Teyssier, I. Iatsunskiy, E. Coy, S. Balme, D. Cornu, P. Miele, N. S. Kalkura, V. Cavailles and M. Bechelany, *ACS Appl. Mater. Interfaces*, 2017, **9**, 33695-33706.

**Keywords:** high temperature thermal conductive, green aqueous method, functional BN nanosheets, polyimide, thermal regulated textile

## TOC

High temperature thermal conductive nanocomposite textile by "green" electrospinning

